Operational Influence Proxies in a TFIM Surrogate: Non-Monotonicity and a Controlled $\omega = 0$ Witness Floor Mechanism

Version 2

Lluis Eriksson
Independent Researcher
lluiseriksson@gmail.com

January 2026 (v1); July 2026 (v2)

Abstract

We study spatial influence detection in a transverse-field Ising chain (TFIM) subjected to localized Markovian noise. Using an operational one-site trace-distance influence proxy computed from TEBD combined with Monte Carlo wavefunction (MCWF) sampling, we test whether remote dissipation produces an identifiable nonzero asymptotic influence offset (a "floor") as a function of separation ϵ. Uncertainties are estimated by trajectory bootstrap and model selection is performed between exponential decay and exponential-plus-offset forms using both BIC and the finite-sample corrected criterion AICc. In the TFIM surrogate regimes explored, we find no robustly identifiable floor for both dephasing and amplitude-damping channels; instead, the influence proxy is non-monotone in separation, consistent with coherent finite-size structure superimposed on average attenuation. To demonstrate that floors can exist as a controlled mechanism independent of fragile spatial fits, we present a Davies/witness stress test: for nonzero zero-frequency bath weight $\gamma(0) > 0$, a commutator witness yields a strictly positive lower bound on an effective decay envelope. Exact-diagonalization calculations show this lower bound is robust to enlarging the observable support and to variations in inverse temperature. *v2 adds:* a synthetic-injection power analysis showing that over the sampled one-octave window $\epsilon \in [16, 32]$ with $n = 5$ points, a constant floor is nearly degenerate with a slow exponential – AICc essentially never detects a floor and even BIC requires $D_0 \sim 30\sigma$ – so "no identifiable floor" is in part a design limitation, now stated as such; a fully declared exact-diagonalization benchmark for the witness (v1 did not record its ED parameters), regenerable from scratch by the shipped suite; a null case showing the witness switches off ($\kappa_{\min} \sim 10^{-29}$) for couplings with vanishing $\omega = 0$ component; an invariant-subspace caveat for the envelope interpretation; and series cross-references.

1 Introduction

Locality constraints in quantum lattice systems limit how quickly and how strongly perturbations influence distant degrees of freedom [1]. Operational influence detection often relies on reduced-state or local-observable proxies rather than direct access to a full many-body channel. A recurring question is whether such proxies exhibit a nonzero asymptotic offset (a "floor") in separation ϵ, or whether they decay without a detectable offset.

This paper has two goals. First, we evaluate a TFIM numerical surrogate using a one-site trace-distance influence proxy under localized Markovian noise, and we test for an identifiable floor using statistically controlled model selection. Second, we provide a controlled stress test in which a floor mechanism exists in a precise sense: as a witness-based lower bound in a Davies-type $\omega = 0$ sector with $\gamma(0) > 0$ [2, 3, 4]. The contrast clarifies a key message: the existence and detectability of floors depends on both the chosen operational proxy and on low-frequency bath structure.

Series context (added in v2). This note is the numerical companion of the $\omega = 0$-floor block of the coherence-maintenance series: the windowed-proxy withdrawal and exact local-sink suppression of 2512.0064 v2 [7] (the non-monotonicity found here is the same phenomenon that motivated that withdrawal), the Davies-class ceiling/floor envelopes of 2512.0070 v2 [8], and the entropic interface 2601.0020 [9], whose Appendix C reproduces Figures 1 and 4 below as illustrations. The proxy-discipline lesson (power analysis before interpreting nulls) follows 2512.0105-style methodology [10].

2 TFIM surrogate: model, proxy, and inference pipeline

2.1 Hamiltonian

We consider a TFIM chain of length N with open boundary conditions and Hamiltonian

$$H = -J \sum_{i=1}^{N-1} X_i X_{i+1} - h \sum_{i=1}^{N} Z_i.$$

(Equivalent to the ZZ–X convention by a global basis rotation.)

2.2 Noise channels and geometry

We study localized Markovian noise applied on a set of sites separated from a probe site S by a distance ϵ: dephasing (jump operators $\propto Z$) and amplitude damping (jump operators $\propto \sigma^- = (X - iY)/2$). For each separation ϵ, noise acts on a small region $\mathcal{N}(\epsilon)$ at distance ϵ from S.

2.3 Operational influence proxy

For each ϵ, we compare (i) a noisy evolution with dissipation at $\mathcal{N}(\epsilon)$ to (ii) a clean unitary evolution under H. With $\bar{\rho}_S^{\text{noisy}}(t)$ the trajectory-averaged reduced state at the probe and $\rho_S^{\text{uni}}(t)$ the unitary reference (independent of ϵ), define the instantaneous trace-distance influence $D_{\text{tr}}(t;\epsilon) := \frac{1}{2}\|\bar{\rho}_S^{\text{noisy}}(t) - \rho_S^{\text{uni}}(t)\|_1$ and windowed aggregates $D_{\text{tr}}^{\mathcal{A}}(\epsilon)$, $\mathcal{A} \in \{\max, \text{mean}, \text{rms}\}$, over post–light-cone windows $t_0(\epsilon) = \alpha\epsilon/v$, $t_1 = t_0 + \tau$.

2.4 Uncertainty estimation and model selection

Uncertainties are bootstrap 16–84% intervals over trajectories. We compare $M_{\text{exp}} : D(\epsilon) = Ae^{-a\epsilon}$ and $M_{\text{floor}} : D(\epsilon) = D_0 + Ae^{-a\epsilon}$ $(A, D_0 \geq 0)$ by weighted least squares with a log-spaced grid over a, summarized by ΔBIC and ΔAICc with BIC $= \chi^2 + k \log n$, AICc $= \chi^2 + 2k + 2k(k+1)/(n-k-1)$ [5, 6]. For the tail-only fits below ($n = 5$), the AICc correction contributes ≈ 18 additional units to the offset model ($k = 3$ vs $k = 2$), so ΔAICc ≈ 20 indicates insufficient support for an extra parameter at small n, not strong physical evidence against D_0.

2.5 Power of the no-floor conclusion (added in v2)

A null is informative only relative to what the design could detect. The suite (Section 5) injects known floors D_0 into synthetic data with the sampled design ($n = 5$, $\epsilon \in \{16, 20, 24, 28, 32\}$, matched noise) and runs the identical pipeline. Result: AICc essentially never selects the floor model (it requires $\Delta\chi^2 > 20$), and even BIC reaches 80% detection only near $D_0 \sim 30\sigma$. The mechanism is a *design degeneracy*: over a one-octave window, a slow exponential ($a \to 0$) mimics a constant offset, so the criteria cannot separate them regardless of sample size. Consequently, the correct reading of Section 3 is: no floor is identifiable *and* the design could not have identified any floor smaller than the in-window signal itself; identifying subdominant floors requires a wider ϵ aspect ratio, amplitude constraints, or channel-specific nulls. This sharpens, rather than weakens, the contrast with the certified witness mechanism of Section 4.

3 TFIM surrogate results

3.1 Dephasing deep tail ($N = 80$, post–LC)

For dephasing at $N = 80$, $\epsilon \in \{16, 20, 24, 28, 32\}$: $D_{\rm tr}^{\mathcal{A}}(\epsilon)$ is non-monotone (a bump appears), indicating coherent finite-size structure superimposed on average attenuation. Model selection yields no supported/identifiable floor for all aggregators: ΔBIC $\approx$ 1.5–1.6, ΔAICc ≈ 20 – i.e. χ^2 improvement ≈ 0 (pure penalty), consistent with no floor signal *within the power limits of Section 2.5.*

3.2 Amplitude damping corroboration ($N = 24$)

At $N = 24$, $\epsilon \in \{2, 4, 6, 8, 10\}$: non-monotone dependence, no-floor model favored across aggregators (ΔBIC ≈ 1.6, ΔAICc ≈ 20), same power caveat.

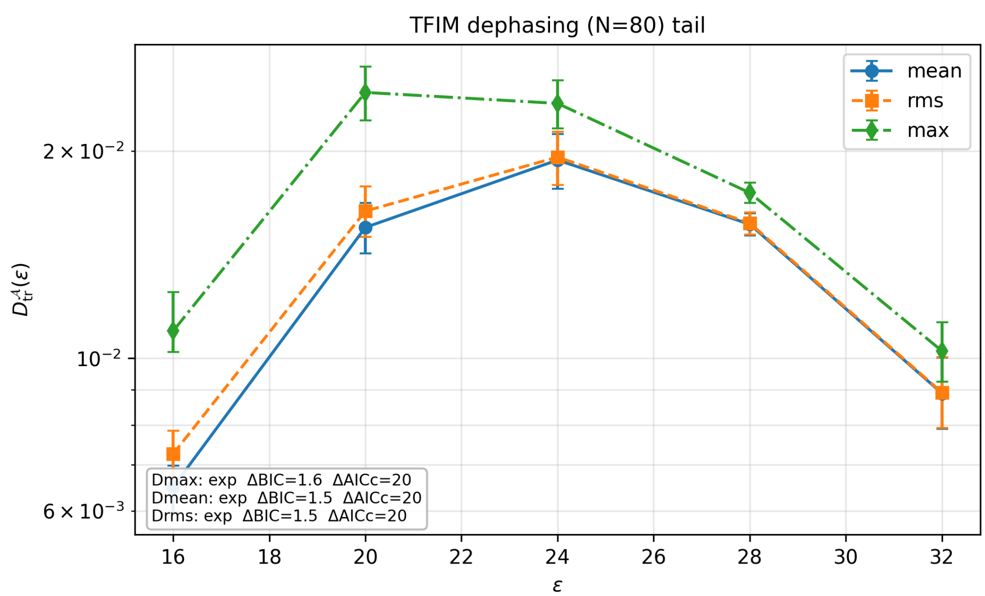

Figure 1: TFIM dephasing tail ($N = 80$): windowed influence proxy with bootstrap 16–84% intervals. Model selection supports the no-floor model for $\mathcal{A} \in \{\max, \text{mean}, \text{rms}\}$; see Section 2.5 for what this does and does not imply.

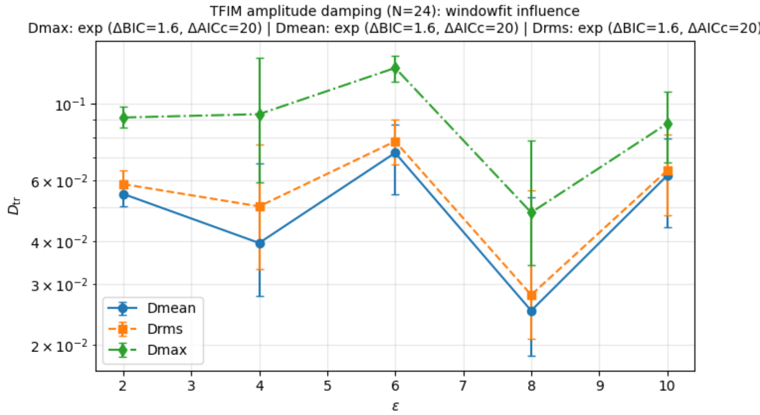

Figure 2: Influence proxy under amplitude damping ($N = 24$); error bars are bootstrap 16–84% intervals. Non-monotone in ϵ.

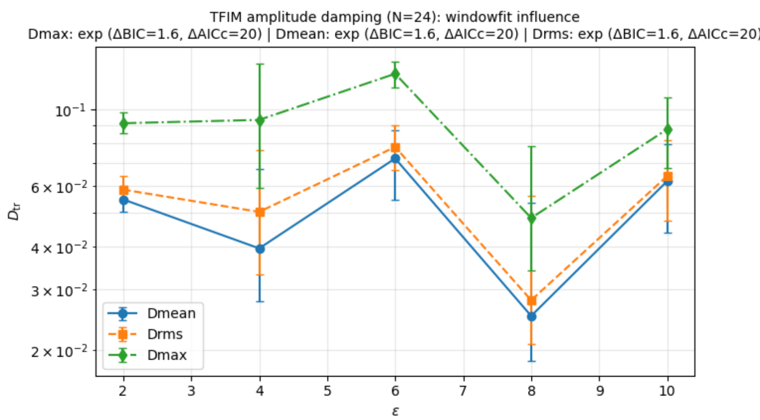

Figure 3: Processed influence summary for the amplitude-damping check ($N = 24$).

Data availability (added in v2). Trajectory-level TEBD/MCWF data are not shipped with this version; the figures are unchanged from v1. The witness computations of Section 4, by contrast, are fully regenerable from scratch by the verification suite.

4 Davies/witness stress test: controlled $\omega = 0$ floor mechanism

4.1 Scope

We use a controlled $\omega = 0$-channel witness (Dirichlet-form identity) as a stress test; we do not reconstruct the full Davies generator. This is a certified lower-bound mechanism statement, not a claim about the full ϵ-dependence of physical decoherence rates in the TFIM surrogate. *(Added in v2)* Moreover, as an instantaneous Dirichlet-ratio bound it controls decay of observables in the witness sector only under the usual invariant-subspace extension (cf. the Grönwall step in 2601.0020 [9]); we use the term "envelope" in that conditional sense.

4.2 Definitions: $S(0)$ and $\mathcal{A}_\epsilon$

With $\{\Pi_n\}$ the spectral projectors of H, define $S(0) := \sum_n \Pi_n S \Pi_n$ (energy-block-diagonal part of the system–bath coupling S); $S(0)$ is generally nonlocal in real space. $\mathcal{A}_\epsilon$ is the span of traceless Pauli strings on a block of length L starting at site $k = j_0 + \epsilon$ (open chain), $j_0 = \lfloor N/2 \rfloor$.

4.3 Witness lower bound

With σ a reference Gibbs/KMS state and $\langle A, B\rangle_\sigma := \mathrm{Tr}(\sigma^{1/2} A^\dagger \sigma^{1/2} B)$,

$$\kappa(\epsilon) \geq \kappa_{\min}(\epsilon) := \frac{\gamma(0)}{2} R_{\mathrm{opt}}(\epsilon), \qquad R_{\mathrm{opt}}(\epsilon) := \max_{O \in \mathcal{A}_\epsilon} \frac{\|[S(0), O]\|_{2,\sigma}^2}{\|O\|_{2,\sigma}^2},$$

so any $R_{\mathrm{opt}}(\epsilon) > 0$ certifies $\kappa_{\min}(\epsilon) > 0$ whenever $\gamma(0) > 0$.

4.4 Exact diagonalization: declared benchmark (revised in v2)

v1 reported ED ranges at $N = 10$ without recording the parameters (J, h, S), which made exact reproduction impossible. v2 fixes a fully declared benchmark, regenerated from scratch by the suite: $N = 10$, $J = 1$, $h = 1.05$, $S = Z$ at the center site, $\gamma(0) = 0.1$, $\epsilon \in \{1, 2, 3\}$, $\beta \in \{0.5, 1, 2\}$, blocks $L \in \{1, 2\}$. The witness-based lower bound ranges

$$\kappa_{\min} \in [1.79 \times 10^{-3}, 5.72 \times 10^{-3}]\ (L = 1), \qquad \kappa_{\min} \in [4.31 \times 10^{-3}, 6.82 \times 10^{-3}]\ (L = 2):$$

strictly positive throughout, increasing with observable support, robust in β – the same qualitative structure as v1's figures (v1's magnitudes are same-order; its exact parameters were not preserved). *Null case (added in v2):* for $S = X$ at the center site the $\omega = 0$ component essentially vanishes and the suite finds $\kappa_{\min} \sim 10^{-29}$: the floor mechanism switches off for couplings with no zero-frequency diagonal part, sharpening the message that low-frequency bath structure – not locality alone – controls floor existence.

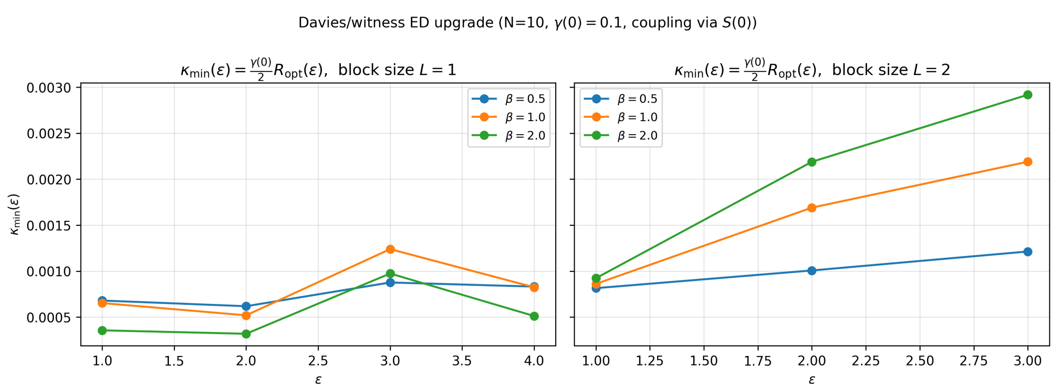

Figure 4: Davies/witness ED ($N = 10$, v1 figure): witness lower bound $\kappa_{\min}(\epsilon) = \frac{\gamma(0)}{2} R_{\mathrm{opt}}(\epsilon)$, $\gamma(0) = 0.1$, for $L = 1, 2$ and $\beta \in \{0.5, 1, 2\}$. See Section 4.4 for the v2 declared benchmark.

5 Verification suite (added in v2)

`verification/2601-0022/verify_2601_0022.py` (pure NumPy/SciPy, ∼70 s): Part A regenerates the declared witness benchmark of Section 4.4 from scratch (ED, KMS inner products, generalized eigenproblem over Pauli blocks) together with the $S = X$ null case; Part B runs the synthetic floor-injection power analysis of Section 2.5 (60 repetitions per injected level, identical fitting pipeline). Reference output ships alongside.

6 Discussion and conclusions

The TFIM surrogate results show that, for this operational one-site trace-distance proxy in the explored regimes, an offset parameter D_0 is not supported/identifiable under either dephasing or amplitude damping – with the v2 power analysis quantifying exactly how strong a floor would have had to be for the design to see it, and identifying the slow-exponential/floor degeneracy of narrow ϵ windows as the limiting factor. The observed non-monotonicity in ϵ indicates coherent finite-size structure that limits the interpretability of strictly monotone envelope fits – the same phenomenon behind the windowed-proxy withdrawal of 2512.0064 v2 [7]. In contrast, the Davies/witness stress test demonstrates an explicit, certified and now exactly reproducible floor mechanism when $\gamma(0) > 0$, which switches off when the coupling lacks a zero-frequency component. Floors are not universal across operational proxies; low-frequency bath structure and the observable family determine whether a floor exists, and the sampling design determines whether it could even be detected.

Note added in v2

No v1 result is retracted: the no-floor model selection, the non-monotonicity, and the positive witness mechanism all stand. v2 adds what a careful referee would demand: (1) the power analysis of Section 2.5 (the no-floor null is design-limited: AICc cannot detect floors at $n = 5$; BIC needs $D_0 \sim 30\sigma$ due to the slow-exponential degeneracy); (2) a fully declared, from-scratch reproducible ED benchmark for the witness (v1's ED parameters were not recorded), with same-order agreement and identical qualitative structure; (3) the $S = X$ null case ($\kappa_{\min} \sim 10^{-29}$); (4) the invariant-subspace caveat on "envelope"; (5) series cross-references and the data-availability statement; (6) Figure 3 caption cleaned.

References

[1] E. H. Lieb and D. W. Robinson, Commun. Math. Phys. **28** (1972) 251–257.

[2] E. B. Davies, Commun. Math. Phys. **39** (1974) 91–110.

[3] H.-P. Breuer and F. Petruccione, *The Theory of Open Quantum Systems*, Oxford University Press (2002).

[4] H. Spohn, J. Math. Phys. **19** (1978) 1227–1230.

[5] K. P. Burnham and D. R. Anderson, *Model Selection and Multimodel Inference*, 2nd ed., Springer (2002).

[6] C. M. Hurvich and C.-L. Tsai, Biometrika **76** (1989) 297–307.

[7] L. Eriksson, ai.viXra:2512.0064 (2025; v2 2026).

[8] L. Eriksson, ai.viXra:2512.0070 (2025; v2 2026).

[9] L. Eriksson, ai.viXra:2601.0020 (2026; v2 2026).

[10] L. Eriksson, ai.viXra:2512.0105 (2025; v2 2026).